A Comparative Spectroscopic Study of Graphene-coated vs Pristine Li(Mn,Ni,Co) Oxide Materials for Lithium-ion Battery Cathodes

Taehoon Kim, Bohang Song, Giannantonio Cibin, Andy Dent, Lu Li and Alexander M. Korsunsky*

***Abstract*— The structural properties of pristine and graphene-coated $Li(Li_{0.2}Mn_{0.54}Ni_{0.13}Co_{0.13})O_2$ materials were studied by the spectroscopic methods, such as Raman spectroscopy, FTIR, and synchrotron XAS. The result from Raman spectroscopy implies that the graphene coating may suppress the monoclinic phase in the pristine material and thus lead to improved stability of the cathode. The combined analyses including the synchrotron XAS have vital implications for developing *in situ* methods to investigate the phase transitions that are related with the stability of the active material and capacity fading during electrochemical cycling of the lithium-ion batteries.**

***Index Terms*—Lithium-layered oxide cathode, spectroscopy, XAS, Raman, FTIR.**

I. Introduction

Lithium layered oxides, which can be represented by the chemical formula $xLi_2MnO_3 \cdot (1-x)LiMO_2$ (M = Mn, Co, and Ni), are one of the most widely used groups of cathode material for the lithium-ion batteries owing to their high theoretical and reversible capacity (over 250 mAh/g), good structural/thermal stability, high discharge capacity, and a range of working voltages allowing for flexible designs [1]. However, a significant issue with this battery type is the irreversible capacity loss during the first charge-discharge cycle that is likely to be related to the structural property changes in the active cathode material (e.g. $Li(Li_{0.2}Mn_{0.54}Ni_{0.13}Co_{0.13})O_2$) . The precise mechanism of the capacity fading process is not clear yet, although several attempts [2]-[4] have been made to reveal the Li^+ reaction mechanism within the active material by investigating phase transitions during the electrochemical cycle. A strong relationship is bound to exist between the electrochemical behavior of batteries and the structural changes of the cathode. It is therefore important to obtain better insight into the structural evolution of the active material in order to improve our understanding of the capacity fading effects attributed to the Li^+ (de)intercalation process.

The major components that constitute the lithium layered oxide cathode are the transition metals such as Mn, Co, and Ni. In the past decades, the spectroscopic method has been widely used to characterize transition metals, particularly in terms of their unique photo-redox and magnetic properties. Especially, synchrotron X-ray absorption spectroscopy (XAS) offers versatile and powerful means of characterizing the cathode material due to its good resolution, element specific sensitivity, and the capability to provide simultaneous analysis of chemical and structural information of the active material. XAS allows the study of the local atomic environment and electronic structure in complicated compounds. Another spectroscopic method, Raman spectroscopy, provides the information on chemical bonding and also possesses great sensitivity to the transition metal oxide catalytic effects. The effects from the strong infrared absorbers such as glass, water, and carbon dioxide being relatively minor, Raman spectroscopy can be utilized to examine phase transitions in the cathode materials for lithium-ion batteries in diverse environments [6]. As a vibrational spectroscopy for the characterization of surface chemistry, Fourier transform infrared spectroscopy (FTIR) has been found useful in a wide range of applications due to its high sensitivity to *in situ* formed single/multiple layers at the solid surface or at the interface between solid and liquid phases. The Attenuated Total Reflectance (ATR) method in FTIR spectroscopy has been proven to be an appropriate method for the study of the formation of solid electrolyte interphase (SEI) on the electrodes in lithium-ion batteries [6]-[7].

Graphene coating of the particles of mixed transition metal oxides has been suggested as a means of improving the electronic conductivity and thus abetting better charging-discharging behaviors [8]. In the present study, the structural properties of pristine and graphene-coated $Li(Li_{0.2}Mn_{0.54}Ni_{0.13}Co_{0.13})O_2$ materials were investigated by Scanning Electron Microscopy (SEM), X-ray diffraction (XRD), Energy-dispersive X-ray spectroscopy (EDX), Raman spectroscopy, FTIR, and synchrotron XAS. The results from the combined spectroscopic and structural

Manuscript received January 03, 2014; revised January 29, 2014. This work was supported in part by the UK Engineering and Physical Sciences Research Council under Grants EP/I020691/1 "Multi-disciplinary Centre for In-situ Processing Studies (CIPS)" and EP/H003215/1 "New Dimensions of Engineering Science at Large Facilities".

Taehoon Kim is a doctoral student, Bohang Song is a post-doctoral researcher and Alexander M. Korsunsky is Professor in the Department of Engineering Science, University of Oxford, Parks Road, Oxford OX1 3PJ, UK. (corresponding author Alexander M. Korsunsky, phone: +441865273043; fax: +441865273010; e-mail: alexander.korsunsky@eng.ox.ac.uk).

Giannantonio Cibin and Andy Dent are with Diamond Light Source, Harwell Oxford Campus, OX11 0DE, U.K.

Lu Li is Professor in the Department of Mechanical Engineering, National University of Singapore, 9 Engineering Drive 1, Singapore 117576.

ISBN: 978-988-19253-3-6
ISSN: 2078-0958 (Print); ISSN: 2078-0966 (Online)

analyses provide the information on the local environment, crystal structure, particle morphology, element distribution, surface chemistry, and oxidation state of the cathode material. This study has vital implications for developing *in situ* methods to examine the phase transitions linked with the capacity fading during electrochemical cycles. As the primary strategic objective, this study serves to shed some light on how to develop high capacity cathodes with enhanced stability for lithium-ion batteries.

II. Experimental

The formula of the active material examined in the present study was $Li(Li_{0.2}Mn_{0.54}Ni_{0.13}Co_{0.13})O_2$ for both pristine and graphene-coated cathodes. The cathode contained 80wt% active material, 10wt% carbon black, and 10wt% PVDF. A spray-dryer assisted sol-gel method was chosen to synthesize the pristine material of $Li(Li_{0.2}Mn_{0.54}Ni_{0.13}Co_{0.13})O_2$. A stoichiometric mixture of metal acetates of Mn, Ni, and Co (molar ratio Mn: Ni: Co = 0.54:0.13:0.13) was dissolved in a 200 mL aqueous solution. The concentration of the metal ions was 0.3 M. The solution was slowly dripped into a 300 mL solution, which was continuously kept stirred, of 3% excess amount of lithium acetate and citric acid as a chelating agent with the identical stoichiometry as the metal ions. A spray-dryer (YC-015, Shanghai Politech Instrument & Equipment Co. Ltd) was used to dry the solution. Further drying was performed on the as-sprayed precursor at 80 ℃ overnight prior to calcination at 800 ℃ for 15 h at a heating rate of 5 ℃ min^{-1}. After the calcination, the powders were cooled down in air. The graphene oxide was prepared by a modified Hummer's method [9]-[12]. The synthesis of graphene oxide onto the surface of the pristine particles was accomplished according to a previously reported method [12]. 0.3g of the as-prepared pristine material was immersed into 30 mL polyallylamine hydrochloride (PAH) solution (1 g L^{-1}) with continuous stirring for 1 h. This was followed by the immersion of the pristine powders in the 15 ml graphene oxide aqueous solution (2 g L^{-1}) with stirring for another 5h. Then, centrifugation was performed and the separated particles were washed 3 times. The washed pristine particles with graphene oxide coating were immersed into L-ascorbic acid (LAA) aqueous solution at 95 ℃ for 30 min with continuous stirring. Finally, the synthesized powder was dried at 80 ℃ overnight. The as-prepared graphene-coated powder was heat treated at 250 ℃ or 350 ℃ for 2h.

Special modified coin cells with X-ray window for *in situ* and *in operando* analysis [2], [4], [14]-[15] were prepared for the X-ray absorption spectroscopy (XAS) analysis. The amount of active material within the cells was measured to be 14.18 mg and 6.58 mg for the pristine (P-cell) and graphene-coated powders (G-cell), respectively. The crystal structure of the powders was analysed by XRD (λ = 1.127 Å). The applied energy was 11.0 keV and the measurement was performed in the 2θ range of 10–90◦. In order to identify the difference of the particle shape between the pristine and graphene-coated powders, SEM was performed with a JEOL JSM-6610LV system. The chemical composition of the active material and its distribution was investigated by the energy dispersive spectroscopy (EDX) within the SEM in order to examine the condition of the synthesized cathode powders. Raman spectroscopy was carried out using a HORIBA HR 800 Dual Microscope with a green laser with 532 nm wavelength to examine the possible presence of multiple chemical phases within the active material. Attenuated Total Reflectance-Fourier transform infrared spectroscopy (ATR-FTIR) was utilized to investigate the surface chemistry and impurity level within the active materials. XAS spectra were collected in transmission mode at the Mn (6.537 keV), Co (7.712 keV), and Ni (8.339 keV) K-edges using a Si (111) double crystal monochromator on the B18 beamline at Dimaond Light Source, Oxford, UK. The size of the beam spot on the cells was approximately 140 x 140 microns and the beam energy was initially calibrated using Mn, Ni, and Co foils. The energy was tuned to the starting values of 7.1 keV, 8.225 keV, and 9.3 keV, for Mn, Co, and Ni analysis respectively. Data interpretation was performed with DEMETER software package [13]. Structural parameters such as the distance between the neighbouring shells, EXAFS Debye–Waller factor ($e^{-2\sigma^2k^2}$), amplitude reduction factor (S_0^2) and the EXAFS R-factor were obtained by fitting within the ARTEMIS application. FEFF 6 algorithm was employed for the fitting with the atomic coordination number (CN) of 6. The error from the edge energy (ΔE_0) was also refined within the application. EXAFS fitting was carried out assuming a two-phase system and the fitting range in the R-space was 1-3.75 Å.

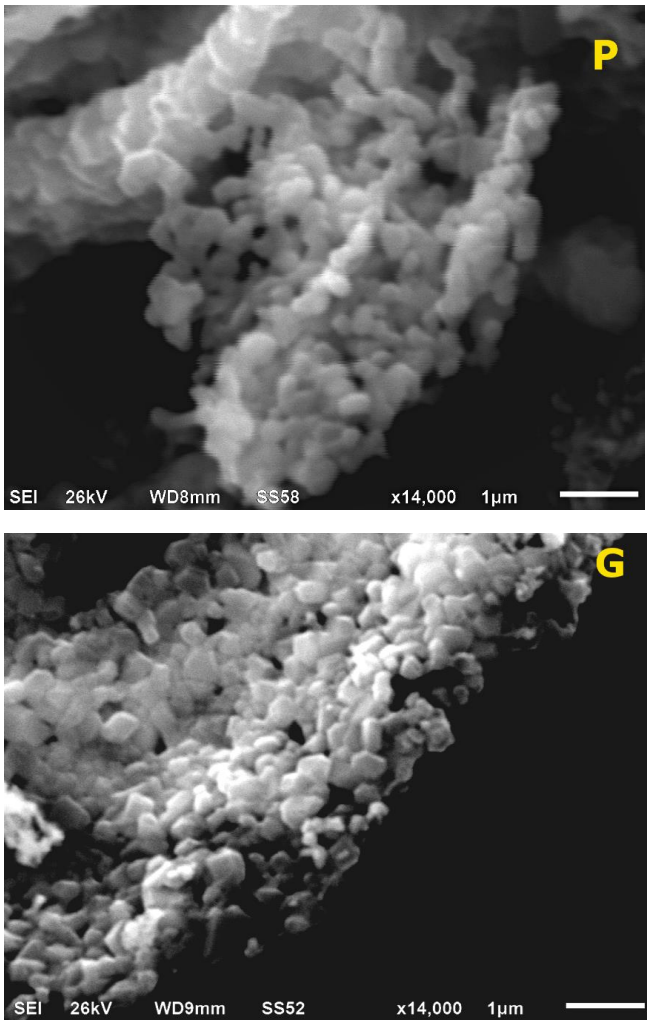

Fig. 1. SEM images of (P) Pristine $Li(Li_{0.2}Mn_{0.54}Ni_{0.13}Co_{0.13})O_2$ and (G) Graphene coated $Li(Li_{0.2}Mn_{0.54}Ni_{0.13}Co_{0.13})O_2$ particles.

ISBN: 978-988-19253-3-6
ISSN: 2078-0958 (Print); ISSN: 2078-0966 (Online)

III. Microscopic Analysis

Fig. 1 compares the images obtained from the SEM analysis on the $Li(Li_{0.2}Mn_{0.54}Ni_{0.13}Co_{0.13})O_2$ cathode materials. The morphology of the powders can be described as an agglomeration of pebble-like particles. There is a slight difference between the pristine and graphene coated particles. More square-shaped particles can be observed in the coated

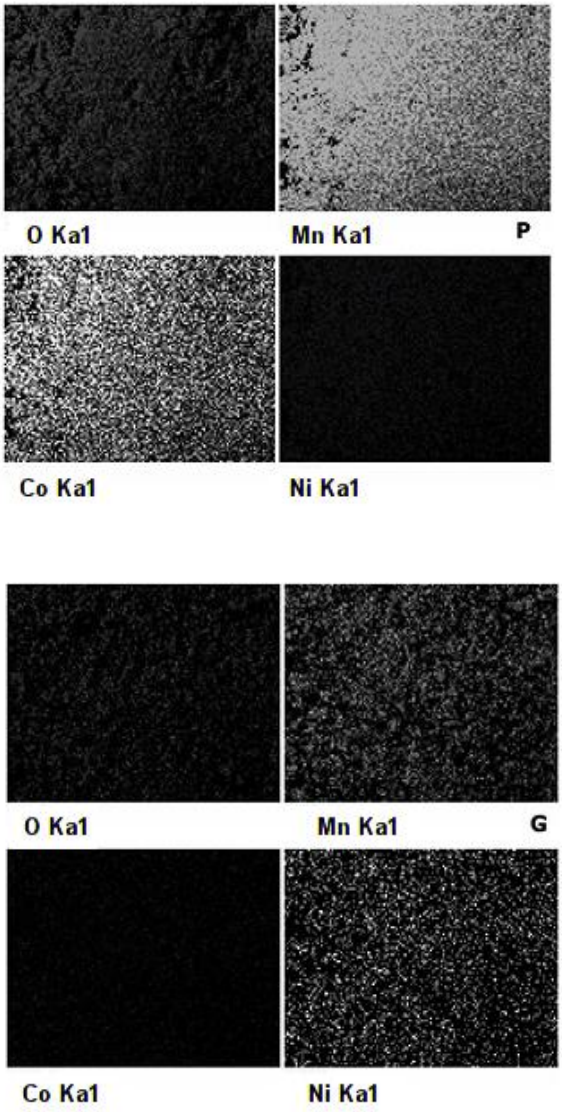

Fig. 2. EDX mapping of O, Mn, Co, and Ni in (P) Pristine and (G) Graphene coated $Li(Li_{0.2}Mn_{0.54}Ni_{0.13}Co_{0.13})O_2$.

powder (G), although the quality of the SEM image is also different due to the improved conductivity of the grapheme-coated material.

The results obtained from the EDX mapping can be seen in Fig. 2. Both the pristine and graphene coated samples reveal a largely homogeneous distribution of the oxygen and transition metal elements, indicating good quality of the chemical synthesis.

Table I presents the results of the EDX quantitative analysis of the cathode powders. The graphene-coated cathode material reveals slightly different stoichiometry compared to the pristine sample. The post-synthesis treatment of the pristine particles could be the one of the reasons for the slight difference in stoichiometry, as well as the presence of graphene/graphene oxide in G-type powders.

TABLE I
EDX Quantitative Analysis of the Active Material

Pristine $Li(Li_{0.2}Mn_{0.54}Ni_{0.13}Co_{0.13})O_2$

Element	Weight%	Atomic%	Relative Stoichiometry
O K	1314.13	69.25	1.772
Mn K	1375.09	21.1	0.54*
Co K	343.31	4.91	0.1256
Ni K	330.26	4.74	0.1213

Graphene-coated $Li(Li_{0.2}Mn_{0.54}Ni_{0.13}Co_{0.13})O_2$

O K	1410.13	73.65	2.241
Mn K	1166.16	17.74	0.54*
Co K	302.55	4.29	0.1305
Ni K	303.74	4.32	0.1314

* Mn was fixed to be 0.54 in the relative stoichiometry.

IV. Diffraction Analysis

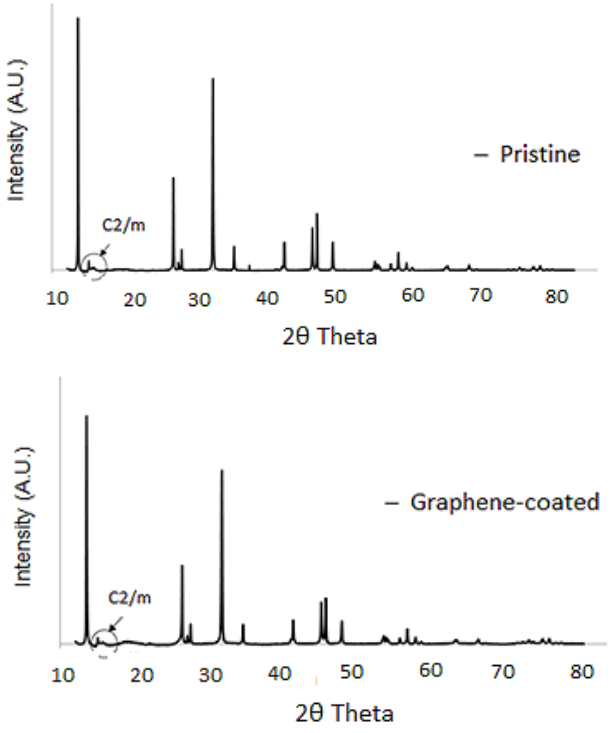

Fig. 3. X-ray diffraction pattern of pristine (top) and graphene-coated powder (bottom) of $Li(Li_{0.2}Mn_{0.54}Ni_{0.13}Co_{0.13})O_2$. Major phase was analysed by Rietveld refinement assuming R-3m symmetry.

The result from the XRD pattern analysis indicates that there are two separate phases present in the active material, as can be seen in Fig. 3. The weak peaks at around 15-16° (2 theta) were attributed to a monoclinic structure (C2/m) of the Li_2MnO_3component in the cathode. The appearance of these peaks is associated with the presence of the $LiMn_6$ cation arrangement in the transition metal layers [1]. However, it remains unclear whether these two phases co-exist as a solid solution of Li_2MnO_3 (C2/m) within $LiMO_2$ (R-3m, M=transition metals), or as an intimate mixture between them. Further work should be done on the investigation of the co-existence state of the phases. Rietveld refinement was performed for the major phase only using the space group R-3m. The refined *a* and *c*-lattice parameters were evaluated to be 2.8557 Å and 14.2572 Å (R_{wp}=4.59%) for the pristine material, respectively. The refined lattice parameters

ISBN: 978-988-19253-3-6
ISSN: 2078-0958 (Print); ISSN: 2078-0966 (Online)

obtained from the graphene-coated material were 2.8574 Å and 14.2584 Å (R_{wp}=3.0%) for the *a* and *c* parameters, respectively. Hence, the calculated *c*/*a* ratios were 4.992 and 4.989 for the pristine and grapheme-coated powders, respectively. The ratio can be used as a reference value for *in situ* XRD studies of the lithium-ion batteries.

V. Raman Spectroscopy

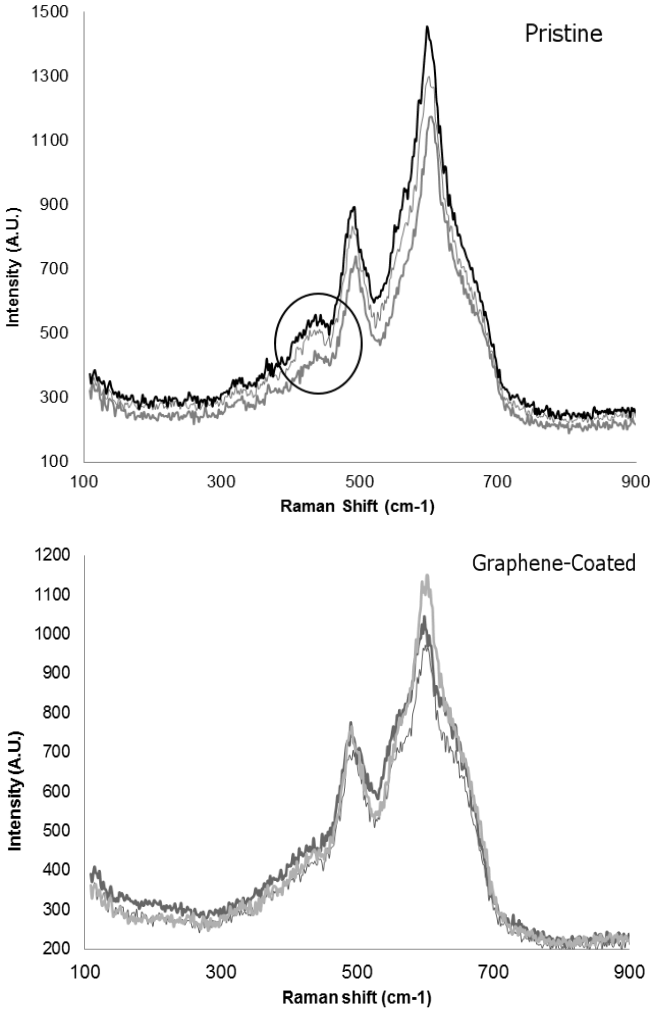

Fig. 4. Raman spectra of the $Li(Li_{0.2}Mn_{0.54}Ni_{0.13}Co_{0.13})O_2$ powders. Each group has been measured from three samples.

Raman spectroscopy is a powerful tool to distinguish different crystal symmetries and hence multiple phases in which the atomic arrangements are closely related [5]. The Raman activity profile for the structure of layered hexagonal rock-salt can be described by the A_{1g} + E_g modes [6]. In the monoclinic structure, the Raman profile must be characterized by three active modes such as $2A_g + B_g$ [6]. The presence of two main peaks approximately at 490 cm^{-1}(E_g) and 600 cm^{-1}(A_{1g}) suggests the hexagonal (R-3m) symmetry in the graphene-coated powders as shown in Fig. 4. They can be assigned to E_g and A_{1g} Raman profiles, respectively. However, there appeared three different peaks in the pristine powders approximately at 440 cm^{-1}, 490 $cm^{-}1$, and 600 cm^{-1} as presented in Fig. 4. The additional peak(s) can be explained by the presence of the monoclinic structure in the pristine material. Presumably, the difference in the Raman analysis between the pristine and graphene-coated samples may be explained by the suppression of the monoclinic phase as a result of post-synthesis treatment differences and the presence of the graphene coating.

VI. FTIR Analysis

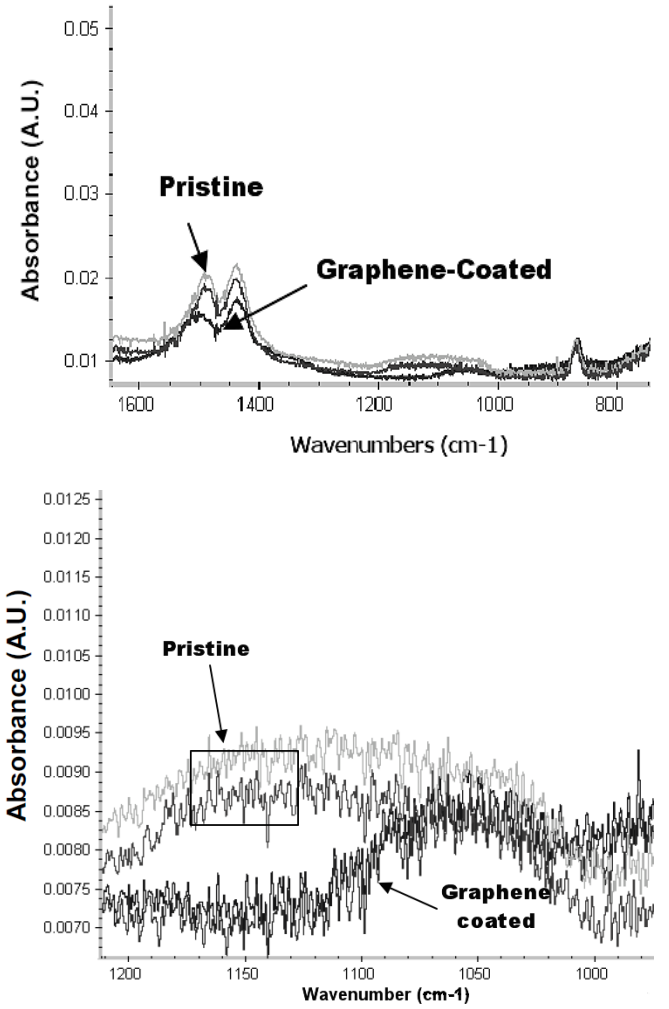

Fig. 5. Attenuated total reflectance FTIR spectra of the pristine and graphene-coated $Li(Li_{0.2}Mn_{0.54}Ni_{0.13}Co_{0.13})O_2$ powders.

Fig. 5 compares the results obtained from the ATR-FTIR analysis of the cathode powders. The two main peaks were observed between 1440 and 1500cm^{-1} in the powders. Those peaks are likely to correspond to the carbon single bond. A closer look at the FTIR spectra indicates a slight difference between the two powder types. This can be perceived from the range 1100 to 1200 cm^{-1} as slightly higher signal has been observed in the pristine powders within this range. This may be explained by the different –C-O stretch of the molecules which may be associated with the graphene coating. Peaks were also observed from 800 to 920 cm^{-1} as shown in Fig. 5. Those peaks can be described by the –C-H bending which is regarded as a strong bond. The presence of –C-H can be explained as the residues from the citric acid during the synthesis process of the active material. Impurities of the cathode material may have influence on the Solid Electrolytes Interphase (SEI) formation at the electrodes and this must be considered as one of the factors contributing to capacity fading in the lithium-ion batteries. Due to the limitation of the FTIR device used, it was not possible to

ISBN: 978-988-19253-3-6
ISSN: 2078-0958 (Print); ISSN: 2078-0966 (Online)

measure the spectra below 620 cm^{-1}. The spectra of Mn-O, Ni-O, and Co-O bonds are expected to be found between 400 and 630 cm^{-1} [16]-[18]. The ATR-FTIR analysis obtained from the coin cells that contain the cathode powders can be seen in Fig. 6. The cells that contain the graphene-coated material were referred to as G-cells, whereas those that contained the pristine material. The observed multiple peaks correspond to the different components present inside the coin cells, namely the cathode, anode, separator, and electrolyte. The reported peaks between 2000 and 2980 $cm^{-1}$are attributed to the C-H bond stretch. This may be explained by the presence of -C-H segments with the Polyvinylidene fluoride (PVDF) binder that constitutes 10% of the cathode. A strong and narrow peak was found around 1700 cm^{-1} in both cell types. This peak is associated with the C=O bond stretch. The appearance of this peak can be ascribed to the ethylene carbonate (EC) and the diethylene carbonate (DEC) in the electrolyte.

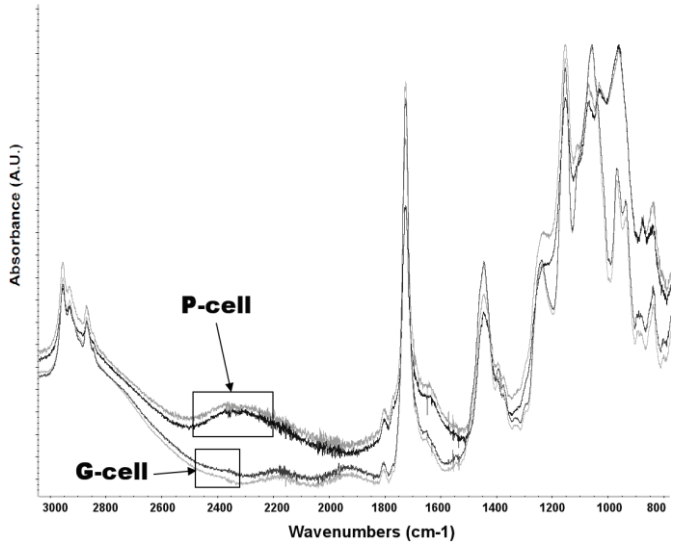

Fig. 6. Attenuated total reflectance FTIR spectra of the pristine and graphene-coated $Li(Li_{0.2}Mn_{0.54}Ni_{0.13}Co_{0.13})O_2$ coin cells. P-cell indicates the coin cell of pristine material, while G-cell indicates the coin cell of graphene-coated material.

In addition, the presence of EC/DEC can result in the appearance of the peak near 1420 cm^{-1}. This peak is attributed to the C-H bond bending, but this data must be interpreted with caution in terms of its origin. Considering the increased intensity of the peak in comparison with the powders, it is highly probable that this peak stemmed from at least two different sources such as the EC/DEC and the residual citric acid from synthesis. We could observe a difference of the FTIR spectra between P-cells and G-cells in the wavelength range 950 to 1100 cm^{-1}. This result was repeatable. These peaks observed from 810 to 1100 cm^{-1} may be attributed to the P-H bond bending, with phosphorous coming from the LiPF6 in the electrolyte. The peaks recorded between 1140 and 1210 cm^{-1} indicate the presence of phosphine oxides (P=O) inside the cell. Regarding the peaks between 1000 and 1200 cm^{-1}, there is another possible interpretation that can be described by the C-F bonds, with the fluorine originated from the PVDF of the cathode. The clear peaks present between 1230 and 1260 cm^{-1} in G-cells are possibly linked with the C-C(O)-C bond stretch. Some of the issues emerging from this finding relate specifically to the development of the *in situ* experiments for the lithium-ion batteries.

VII. XAS

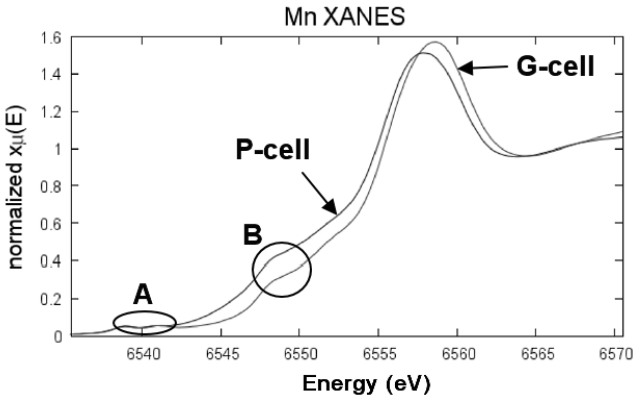

Fig. 7. Normalised XANES spectra (k^3-weighted) at Mn K-edge of the $Li(Li_{0.2}Mn_{0.54}Ni_{0.13}Co_{0.13})O_2$ on G cell and P-cell.

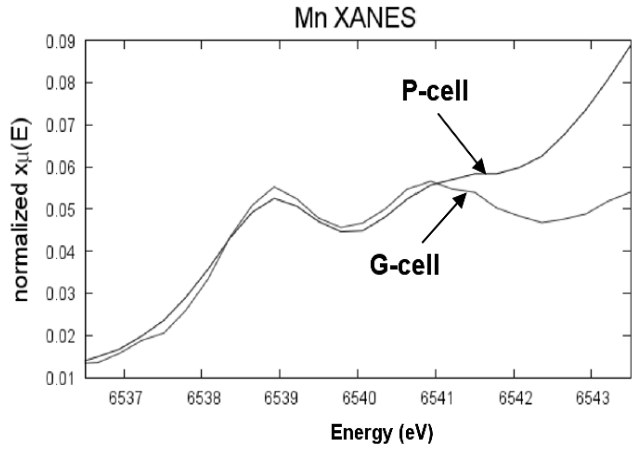

Fig. 8. Double-peaks in Mn K pre-edge of P-cell and G-cell.

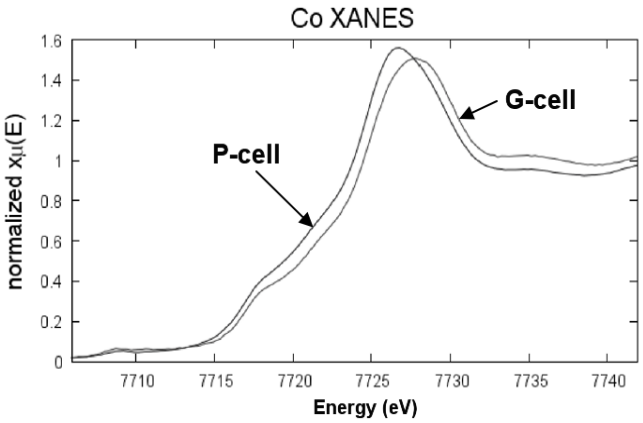

Fig. 9. Normalised XANES spectra (k^3-weighted) at Co K-edge of the $Li(Li_{0.2}Mn_{0.54}Ni_{0.13}Co_{0.13})O_2$ on G cell and P-cell.

The normalized XANES spectra of the Mn K edge for the P-cell and G-cell are presented in Fig. 7. P-cell contains the $Li(Li_{0.2}Mn_{0.54}Ni_{0.13}Co_{0.13})O_2$ pristine powder, whereas G-cell contains the $Li(Li_{0.2}Mn_{0.54}Ni_{0.13}Co_{0.13})O_2$ graphene-coated powder. The Mn K-edge XANES patterns of both cells were similar. There were two significant indications of the absorption phenomena (A, B) as shown in Fig. 7. Absorption phenomenon B can be associated with the electric dipole

ISBN: 978-988-19253-3-6
ISSN: 2078-0958 (Print); ISSN: 2078-0966 (Online)

transition from 1*s* to 4*p* via a shakedown process. Absorption phenomenon A (in Fig.7) indicates the double pre-edge peaks of Mn K-edge, showed magnified in Fig. 8. Those peaks can be assigned to the 1*s*-3d_{t2g} (lower energy) and the 1*s*-3d_{eg} (higher energy) transitions that are formally dipole-forbidden in a centrosymmetric system.

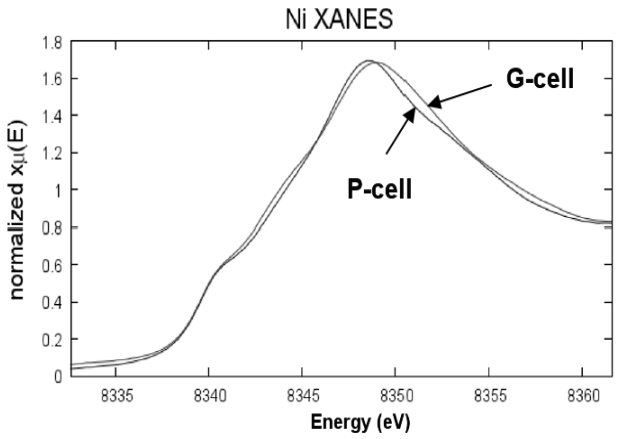

Fig. 10. Normalised XANES spectra (k^3-weighted) at Ni K-edge of the $Li(Li_{0.2}Mn_{0.54}Ni_{0.13}Co_{0.13})O_2$ on G cell and P-cell.

These peaks can arise from a weak quadrupole transition or the 3*d*-4*p* orbital hybridization from the loss of centrosymmetric environment caused by the distortion of the octahedral 3a site in the R-3m structure. Fig. 9 shows the normalized XANES spectra of the Co K edge for the P-cell and G-cell. Fig. 10 compares the XANES spectra of the cells at the Ni K-edge. G-cell and P-cell showed very similar spectra indicating similar local environment and chemical oxidation state. The clear spectra obtained from the coin cells demonstrate the suitability of our specially designed coin cells for high precision *in situ* and *in operando* studies of Li ion batteries.

TABLE II
EXAFS FITTING OF MN, CO, AND NI

Bond	Bond length (Å)	R-range (Å)	σ^2 (Å^2)	ΔE_0 (eV)	R-factor
P-cell					
Mn-O	1.90841	1-3.6	0.00275	5.863	0.019
Co-O	1.92972	1-3.6	0.004	7.98	0.014
Ni-O	2.04076	1.25-3.5	0.005	5.077	0.02
G-cell					
Mn-O	1.90780	1-3.75	0.00226	4.666	0.014
Co-O	1.92979	1-3.75	0.00385	5.461	0.010
Ni-O	2.03966	1.1-3.7	0.00261	1.037	0.020

Fig. 11 shows the k^3-weighted Fourier transforms of the Mn, Co, and Ni K-edges of $Li(Li_{0.2}Mn_{0.54}Ni_{0.13}Co_{0.13})O_2$ in the G-cell and P-cell in R-space. The local atomic arrangements were interpreted by EXAFS. The coordination number of 6 was used for the calculation of the Mn-O, Co-O, and Ni-O bond lengths. The EXAFS results with the fitting parameters can be seen in Table II.

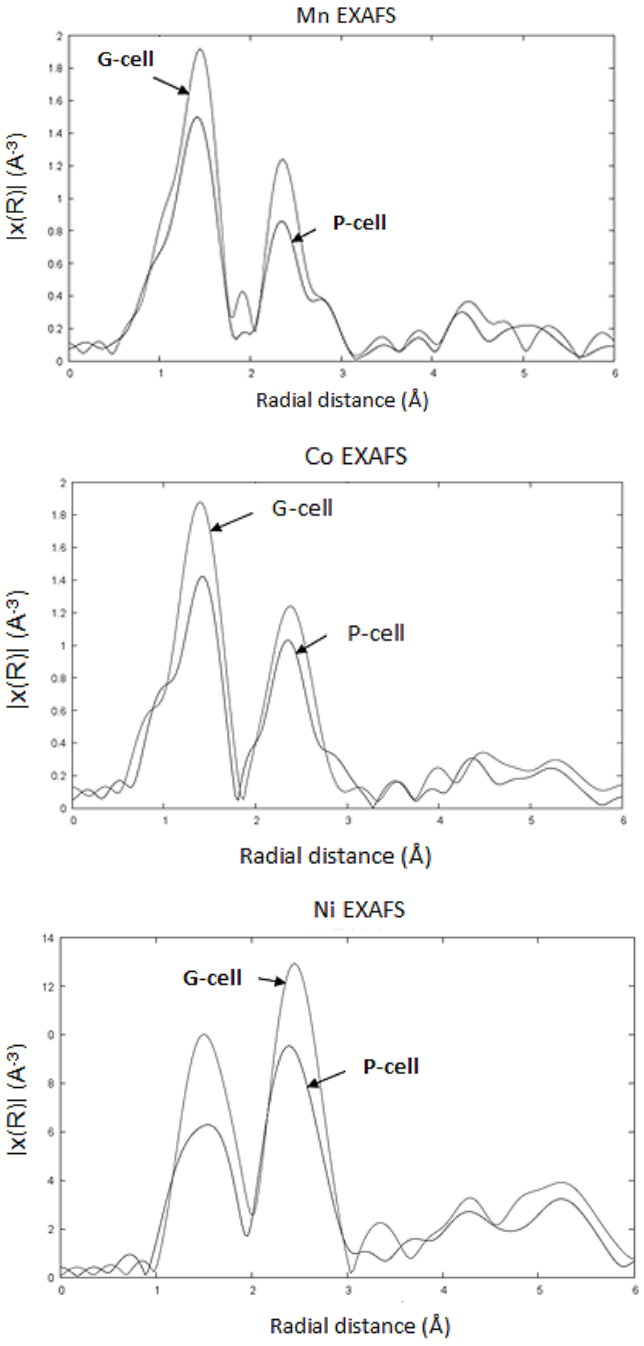

Fig.. 11. k^3-weighted Fourier transform magnitudes of K-edge Mn, Co, and Ni spectra of G-cell and P-cell in R-space.

VIII. DISCUSSION AND CONCLUSIONS

Several structural characterization methods were employed in this study to analyse mixed-oxide cathode materials for Li-ion batteries, namely, XRD, EDX in SEM, Raman spectroscopy, FTIR, and synchrotron XAS. In agreement with the overall trigonal structure (space group R-3m), XRD revealed the presence of the monoclinic phase (space group C2/m) in both cathode powders. The result obtained from the Raman spectroscopy suggests the graphene coating on the lithium-layered oxide material ($Li(Li_{0.2}Mn_{0.54}Ni_{0.13}Co_{0.13})O_2$) may reduce the appearance of the monoclinic structure in the cathode. The quality of chemical synthesis of the powders was revealed by EDX and FTIR. The graphene-coated material showed better accuracy

ISBN: 978-988-19253-3-6
ISSN: 2078-0958 (Print); ISSN: 2078-0966 (Online)

in terms of the chemical stoichiometry than that of the pristine material.

Clear XANES spectra could be obtained from our specially modified coin cells. XANES can provide the information of the oxidation states of the transition metals and the symmetry of the crystal structure. EXAFS fitting was successfully performed on both types of coin cells. The results from the EXAFS computation indicate similar local atomic environment in the P-cell and G-cell.

The current study demonstrated the great potential of the spectroscopic methods for *in situ* and *in operando* phase transition studies. These form a key research theme that needs to be pursued in order to improve the stability of lithium-layered oxide cathode materials.

ACKNOWLEDGMENTS

The authors acknowledge beamtime allocation on the B18 Core EXAFS beamline at Diamond Light Source (DLS, UK) under the rapid access scheme with proposal number SP 4004, as well as the use of the facilities at the Research Complex at Harwell (RCaH).

AMK wishes to acknowledge the support of EPSRC through grants EP/I020691 "Multi-disciplinary Centre for In-situ Processing Studies (CIPS)", EP/G004676 "Micromechanical Modelling and Experimentation", and EP/H003215 "New Dimensions of Engineering Science at Large Facilities".

REFERENCES

[1] Thackeray, M.M., Kang, S.-H., Johnson, C.S., Vaughey, J.T., Benedek, R. and Hackney, S.A. (2007), "Li2MnO3-stabilized LiMO2 (M = Mn, Ni, Co) electrodes for lithium-ion batteries", Journal of Materials Chemistry, Vol. 17 No. 30, p. 3112.

[2] Ito, A., Sato, Y., Sanada, T., Hatano, M., Horie, H. and Ohsawa, Y. (2011), "In situ X-ray absorption spectroscopic study of Li-rich layered cathode material Li [Ni0.17Li0.2Co0.07Mn0.5]O2," *Journal of Power Sources*, Vol. 196 No. 16, pp. 6828–6834.

[3] Bareño, J., Balasubramanian, M., Kang, S.H., Wen, J.G., Lei, C.H., Pol, S.V., Petrov, I., et al. (2011), "Long-Range and Local Structure in the Layered Oxide Li 1.2 Co 0.4 Mn 0.4 O 2," Chemistry of Materials, Vol. 23 No. 8, pp. 2039–2050.

[4] Simonin, L., Colin, J.-F., Ranieri, V., Canévet, E., Martin, J.-F., Bourbon, C., Baehtz, C., et al. (2012), "In situ investigations of a Li-rich Mn–Ni layered oxide for Li-ion batteries," Journal of Materials Chemistry, Vol. 22 No. 22, pp. 11316–11322.

[5] Hwang, S.-J., Park, H.-S., Choy, J.-H., Campet, G., Portier, J., Kwon, C.-W. and Etourneau, J. (2001), "Micro-Raman Spectroscopic Study on Layered Lithium Manganese Oxide and Its Delithiated/Relithiated Derivatives," Electrochemical and Solid-State Letters, Vol. 4 No. 12, pp. A213–A216.

[6] Baddour-Hadjean, R. and Pereira-Ramos, J.-P. (2010), "Raman Microspectrometry Applied to the Study of Electrode Materials for Lithium Batteries," Chemical Reviews, Vol. 110 No. 3, pp. 1278–1319.

[7] Chagnes, A. and Swiatowska, J. (n.d.). "Electrolyte and solid-electrolyte interphase layer in lithium-ion batteries," Lithium Ion Batteries-New Developments, pp. 145–172.

[8] He, Z., Wang, Z., Guo, H., Li, X., Xianwen, W., Yue, P. and Wang, J. (2012), "A simple method of preparing graphene-coated Li [Li 0.2Mn0.54Ni0.13Co0.13]O2 for lithium-ion batteries," Materials Letters.

[9] Si, Y. and Samulski, E.T. (2008), "Synthesis of water soluble graphene", Nano letters, Vol. 8 No. 6, pp. 1679–1682.

[10] Gómez-Navarro, C., Weitz, R.T., Bittner, A.M., Scolari, M., Mews, A., Burghard, M. and Kern, K. (2007), "Electronic transport properties of individual chemically reduced graphene oxide sheets", Nano letters, Vol. 7 No. 11, pp. 3499–3503.

[11] Hummers, W.S. and Offeman, R.E. (1958), "Preparation of Graphitic Oxide", Journal of the American Chemical Society, Vol. 80 No. 6, pp. 1339–1339.

[12] Zhou, W., Zhu, J., Cheng, C., Liu, J., Yang, H., Cong, C., Guan, C., et al. (2011), "A general strategy toward graphene@metal oxide core–shell nanostructures for high-performance lithium storage", Energy & Environmental Science, Vol. 4 No. 12, pp. 4954–4961.

[13] B. Ravel and M. Newville (2005), "ATHENA and ARTEMIS: data analysis for X-ray absorption spectroscopy using IFEFFIT," Journal of Synchrotron Radiation 12, pp. 537–541.

[14] Deb, A., Bergmann, U., Cramer, S.P. and Cairns, E.J. (2005), "In situ x-ray absorption spectroscopic study of the LiNi1/3Co1/3Mn1/3O2 cathode material," Journal of Applied Physics, Vol. 97 No. 11, pp. 113523–113523.

[15] Mohanty, D., Kalnaus, S., Meisner, R.A., Rhodes, K.J., Li, J., Payzant, E.A., Wood, D.L., et al. (2013), "Structural transformation of a lithium-rich Li1.2Co0.1Mn0.55Ni0.15O2 cathode during high voltage cycling resolved by in situ X-ray diffraction," Journal of Power Sources, Vol. 229, pp. 239–248.

[16] Jeong, S.K., Song, C.-H., Nahm, K.S. and Stephan, A.M. (2006), "Synthesis and electrochemical properties of Li[Li0.07Ni0.1Co0.6Mn0.23]O2 as a possible cathode material for lithium-ion batteries," Electrochimica Acta, Vol. 52 No. 3, pp. 885–891.

[17] Zheng, J., Deng, S., Shi, Z., Xu, Hongjie, Xu, Hui, Deng, Y., Zhang, Z., et al. (2013), "The effects of persulfate treatment on the electrochemical properties of Li[Li0.2Mn0.54Ni0.13Co0.13]O2 cathode material," Journal of Power Sources, Vol. 221, pp. 108–113.

[18] Singh, G., West, W.C., Soler, J. and Katiyar, R.S. (2012), "In situ Raman spectroscopy of layered solid solution Li2MnO3–LiMO2 (M = Ni, Mn, Co)," Journal of Power Sources, Vol. 218, pp. 34–38.